

THE USE OF UNMANNED AERIAL VEHICLE (UAV) REMOTELY SENSED DATA AND BIOPHYSICAL VARIABLES TO PREDICT MAIZE ABOVE-GROUND BIOMASS (AGB) IN SMALL-SCALE FARMING SYSTEMS

#11068

¹*Celuxolo M Dlamini, ¹John Odindi, ¹Onesimo Mutanga, ²Trylee N Matongera

¹Discipline of Geography and Environmental Science, School of Agricultural Earth and Environmental Sciences, University of KwaZulu-Natal, Scottsville, Pietermaritzburg 3209, South Africa; ²Centre for Transformative Agricultural and Food Systems, School of Agricultural, Earth and Environmental Sciences, University of KwaZulu-Natal, Scottsville, Pietermaritzburg 3209, South Africa

*e-mail: 219003508@stu.ukzn.ac.za/celuxolomichal09@gmail.com; +27780632013

ABSTRACT

Considering the current and projected increase in human population, approaches to optimize crop productivity to meet the rising demand are paramount. Timely and accurate maize Above Ground Biomass (AGB) measurements allow for development of models that can precisely predict yield prior to harvesting, useful for food production management and sustenance. The development of Unmanned Aerial Vehicles (UAVs) as a new generation of robust remote sensing platforms, mounted with high-resolution sensors has allowed timely and accurate prediction of maize AGB in pursuit of sustaining food security. This study aimed to predict maize crop AGB in small-scale farming systems using UAV-remotely sensed data and landscape biophysical variables. The DJI Matrice 300 UAV mounted with a MicaSense multispectral camera was used to acquire high-resolution images at four phenological stages that covered the vegetative (V8 & V12) and reproductive stages (R2 & R5). Furthermore, in-situ plant biophysical measurements and landscape variables were acquired and combined with UAV-remote sensing derived vegetation indices to model maize AGB using a Deep Neural Network (DNN) model. Results showed that the V12 phenological stage yielded a better overall prediction accuracy ($R^2 = 0.74$) than the V8 ($R^2 = 0.65$), R2 ($R^2=0.71$), and R5 ($R^2=0.67$) phenological stages. The study concludes that the V12 and R2 phenological stages are optimum for estimating maize AGB. This study contributes to a better understanding of maize crop health and crop monitoring efforts for improved food security.

Keywords: UAV-Remote Sensing; Above-Ground Biomass; Maize; Smallholder Farming; Deep Neural Networks.

INTRODUCTION

Small-scale crop farming plays a critical role in the economies of developing countries and is crucial for sustaining food security. However, productivity in smallholdings is often adversely affected by unfavourable bioclimatic conditions, climate change, and lack of farming resources (Mgbenka et al., 2016). Maize (*Zea mays*) is ranked as one of the most extensively cultivated crops worldwide. In South Africa, maize is widely produced and consumed as a staple food by the majority population and also used for livestock fodder (Luo et al., 2019; Ngoune Tandzi & Mutengwa, 2019). Other uses of maize include the production of starch, ethanol, and fuels (Mgbenka et al., 2016). Although the demand for maize has significantly increased in South Africa,

challenges related to production and yield remain prevalent (Haarhoff et al., 2020; Verschuur et al., 2021). Hence, it is imperative to adopt prompt and robust techniques such as crop yield prediction to accurately counteract these challenges.

Maize Above Ground Biomass (AGB) is an essential basis for crop yield formation as it indicates plant growth and productivity (Meiyan et al., 2022; Tang et al., 2023). A higher maize AGB signifies a superior crop performance in capturing and converting sunlight, nutrients, and water into energy for grain development and increased yield (Luo et al., 2019). A direct positive correlation between maize AGB and yield is well established in literature (Leroux et al., 2019; Tollenaar & Lee, 2002; Zhang et al., 2021). Hence, timely and accurate maize AGB measurements allow for development of models that can precisely predict yield prior to harvesting, useful for strategic evaluations, financial planning, efficient irrigation, and food production management (Yahui Guo et al., 2020). Furthermore, maize AGB serves as a crucial source of nutrition for livestock during periods of limited forage availability, such as the dry season (Palacios-Rojas et al., 2020). Therefore, the assessment of maize AGB to optimise yield, particularly in small-scale farming systems, is essential for optimising productivity and mitigating potential losses (Cheng et al., 2020).

Traditionally, quantifying maize AGB involves in-situ measurements of foliar weight, which is destructive and laborious, hence unsuitable for large spatial extents and repeated observations (Gerke, 2019; Han et al., 2019b). Recently, satellite remote sensing has been widely adopted to accurately monitor agricultural crops, with many studies showing a positive correlation between remotely sensed variables and AGB (Battude et al., 2016; Kayad et al., 2019; Leroux et al., 2019). For instance, Geng et al. (2021) estimated maize AGB using Moderate Resolution Imaging Spectroradiometer (MODIS) reflectance data and machine learning, achieving a coefficient of determination of 0.77 ($R^2 = 0.77$). However, despite these successes, the application of satellite remote sensing is limited by as among others cloud cover, which significantly restricts maize crop monitoring requirements for small-scale farming systems (Zhang et al., 2021). Furthermore, small-scale farming systems are characterized by small spatial extents of less than two hectares, hence higher spatial resolution sensors are necessary for effective capture of crops spectral information (Peter et al., 2020). In addition, the transition between phenological stages in maize crops occurs rapidly, necessitating the use of high-temporal-resolution sensors and on demand dataset to accurately monitor and capture the changes in AGB at each growth stage (B. Yang et al., 2022).

Recently, Unmanned Aerial Vehicles (UAVs), also known as drones, have demonstrated a remarkable capability to bridge the gap between satellite remote sensing and ground-based observations (Gargiulo et al., 2023). This is attributed to their ability to provide cloud-free, near-real-time data at ultra-high spatial resolution (Z. Li et al., 2022; Sharma et al., 2022). UAVs offer several benefits for agricultural crop monitoring that include the ability to hover over areas of interest and fly beneath cloud cover at flexible altitudes, allowing for high resolution imagery and precise monitoring of individual crops (Aasen et al., 2018). Additionally, their flexible flight mission make them ideal for capturing data during optimal periods, such as the short-window peak photosynthetic phase in maize crops (B. Yang et al., 2022). However, despite these advancements and capabilities, studies on the use of UAV technology on small holder farms, particularly in the global south, remain scarce. This underscores the need for studies that investigate the potential of UAVs, equipped with high resolution sensors, in predicting maize AGB in small-scale farming systems.

High resolution sensors mounted onto UAV platforms cover a wide range of the electromagnetic bands including the visible, near-infrared, and red-edge sections that are useful in predicting maize AGB and deriving vegetation indices to support yield estimations (Li et al., 2016). For instance, vegetation indices derived from the near-infrared and red-edge wavelengths such as the Normalized Difference Vegetation Index (NDVI), have demonstrated the ability to detect subtle changes in crops properties such as canopy structure, photosynthetic activity, and crop health (Che et al., 2022; Vélez et al., 2023). For example, Brewer et al. (2022) obtained satisfactory results by using various multispectral derived vegetation indices such as NDVI and Soil Adjusted Vegetation Index (SAVI) for estimating leaf chlorophyll content to determine crop health and vigour.

Typically, maize crops are characterised by variable stock height, density, and greenness, while canopy vegetation index remains unchanged (Adewopo et al., 2020). Hence, vegetation index-based empirical approaches alone cannot accurately estimate maize AGB. Consequently, to account for these variations, biophysical variables such as leaf chlorophyll content and leaf area index (LAI) can be combined with vegetation indices to accurately predict maize AGB (Meiyan et al., 2022). Leaf chlorophyll content and LAI have been identified as strong crop health indicators that positively correlate with maize AGB (Che et al., 2022; Liu et al., 2019; Luo et al., 2019). However, measuring the aforementioned biophysical variables is only ideal for small spatial extents (Liu et al., 2023). In addition, considering that most small-scale farmlands are often characterized by challenging terrain featuring steep topography, it is essential to assess the influence of landscape variability on maize AGB (Polzin & Hughes, 2023). Therefore, landscape and landscape related variables that directly and indirectly influence crop growth such as soil moisture, slope, aspect, and elevation can provide a precise maize AGB estimation (Fry & Guber, 2020; Goldenberg et al., 2022; Svedin et al., 2021). Consequently, integrating drone-derived multispectral bands, with optimal vegetation indices, and biophysical landscape variables can provide better and precise estimates of maize AGB in small-scale farming systems.

Numerous regression techniques have been proposed in literature for the prediction of crop properties (Ali et al., 2022; Khan et al., 2022; Tripathi et al., 2022). Machine learning algorithms, combined with spectral variables from remote sensing datasets have proven superior for data analysis than other statistical approaches (Altaweel et al., 2022). Deep learning algorithms, such as Deep Neural Networks (DNN), have particularly gained popularity over the past decades for their ability to learn and discover patterns from large and complex datasets and generate accurate predictions (X. Li et al., 2022; Muruganatham et al., 2022). DNN comprises a hierarchy of more than two hidden neural network layers and are subsequently called ‘deep learning’ (Odebiri et al., 2021a, 2021b). The primary limitation of this technique is its propensity to overfitting and requirement of large datasets for optimal performance (Cao et al., 2022). However, features such as regularization and dropout in neural networks can counteract these effects (Vojnov et al., 2022). Numerous studies have successfully adopted DNN to predict maize agronomic variables and obtained results surpassing other machine learning algorithms (Khaki & Wang, 2019; Lischeid et al., 2022). Despite its potential, deep learning is the least used approach in agricultural monitoring applications, particularly at small-scale extents due to small acquirable datasets. Therefore, there is need for further research to explore the full potential of UAV remotely sensed data combined with landscape and biophysical variables for estimating and mapping maize crop AGB using DNN machine learning techniques.

Studies have employed either plant biophysical, landscape variables or remotely sensed data to estimate maize AGB (Liu et al., 2019; Luo et al., 2019; Meiyan et al., 2022). Generally, studies have seldom integrated the two, with the landscape variables for precision agriculture. Therefore, this study sought to evaluate the utility of UAV remotely sensed data combined with landscape and biophysical variables in estimating maize AGB in small-scale farming systems using DNN machine learning techniques. The main objective of this study was to predict maize AGB using a combination of UAV remotely sensed data, landscape variables, and plant biophysical variables. Additionally, this study sought to determine the optimum phenological stage for timely and efficient maize AGB prediction in subsequent seasons. Finally, the study sought to assess the performance of DNN algorithm to identify an optimal model for predicting maize AGB using small spatial extent acquired dataset.

MATERIALS AND METHODS

Description of the study area

This study was conducted in Swayimane communal area (Latitude: -29.524444°, Longitude: 30.699846°) within the UMshwathi Municipality, in the KwaZulu-Natal province, South Africa (Fig.1). The experimental field is approximately 1.4 hectares and exhibits distinct variations in slope, aspect, and elevation. Average air temperature is 17 °C, while the minimum and maximum temperatures are 11.8 °C and 24 °C, respectively (Ndlovu et al., 2021) . Annual rainfall ranges from 600 mm to 1100 mm, with most rainfall received in summer. Swayimane is characterized by wet-hot summers and dry-cold winters. Since cropping activities in the study area are rain fed, crops are grown during the summer season. The area has excellent bioclimatic and physical conditions, that include loam soils with efficient nutrient and water holding capacity as well as optimum terrain for efficient sunlight capture, making it suitable for crop farming. Farmers in the area mainly rely on traditional farming methods such as use of kraal manure as fertilizers and animal draft implements for ploughing and weeding. However, with recent socio-economic improvements in the area, some farmers are adopting artificial fertilizers and mechanized farming, particularly in larger fields. In addition to maize, legumes, sweet potatoes, taro and small holding sugarcane are grown in the study area.

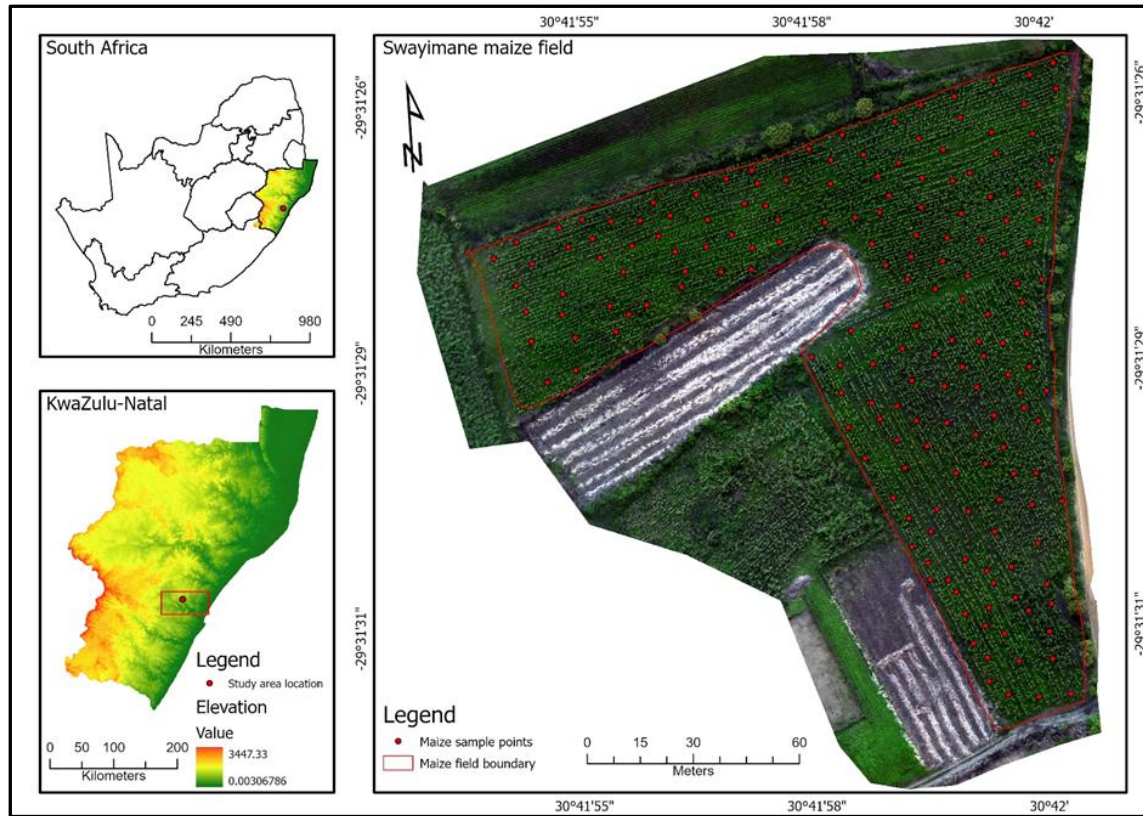


Figure 1. Location of the study site.

Maize phenotyping

The maize field was planted with the SC 701 hybrid (Pannar Seed Company, SA) on the 24th of February 2023, and harvested on the 7th of July 2023. The SC 701 seed type was chosen because of its high yield capacity estimated at more than 13 tons per hectare according to the seed producers. The SC 701 hybrid is late maturing (140-148 days) and known to be heat and drought tolerant. However, in such cases, irrigation is recommended for maximum yield. The maize was rain-fed throughout the growing season, and no drought and extreme temperatures were recorded. The maize was planted in rows perpendicular to the slope to minimize nutrient runoff and soil erosion during rainfall. The distance between the crops and rows was at least 20 cm and 70 cm, respectively, to avoid inter-competition within the crops and stunted growth. To eradicate weeds, an affordable water-soluble Basagran herbicide with a mixability of 480 g/l was applied when the maize was 30 days old, and a nitrogen-phosphorus-potassium [N: P: K (2:3:4=30)] fertilizers applied when the maize was 50 days old to enhance growth.





Data acquisition

Ground data collection

Data for the study was collected at four phenological stages ranging from the vegetative to reproductive growth phases i.e. V8 (32 days old), V12 (47 days old), R2 (96 days old) and R5 (123 days old) (Table 1). The vegetative stages were selected as they are characterized by fully developed leaves, which is essential for field measurements and light reflectance. The R2 is full canopy stage while R5 represents the end of mass gain in maize crop. Field measurements were

conducted at four-week intervals to capture the above-mentioned stages of the growth cycle. Using a handheld Trimble Global Positioning System (GPS), 200 points were sampled using a stratified random approach within the experimental plot. The experimental plot was divided into sub strata based on slope, crop health, and crop size. Thereafter, random crops within the strata were sampled, ensuring variability capturing and a comprehensive and representative sample of the maize population. The approach was adopted to capture the size variability and representative crops for the whole maize field. Each sample point was marked with red tape and labelled for consistent monthly measurements. Field measurements were conducted on clear sunny days between 10 a.m. and 14:00 p.m. to capture data at peak photosynthetic activity and maximum reflectance.

Table 1. Maize phenological stages used in the study.

Growth Stage	Vegetative Stages	
	V8	V12
Day after sowing	32	47
Maize Crop		
Growth Stage	Reproductive stages	
	R2	R5
Day after sowing	96	123
Maize Crop		

At each sampling point, LAI was obtained using a LiCOR 2200C plant canopy analyser (LI-COR GmbH, Germany). The analyser uses 7°, 22°, 38°, 52°, and 68° zenith angles to measure light

interception and transmittance below and above the plant canopy and ultimately estimates the LAI (Buthelezi et al., 2023). Soil moisture content was measured using HH2 moisture probe (Delta-T soil moisture sensors, United states) at each sample point. The HH2 soil moisture probe is inserted in the soil close to the root systems of the crop and records soil moisture volume with a 5% accuracy based on standard calibration (Cheng et al., 2022). Leaf chlorophyll content was measured using a Konica Minolta Soil Plant Analysis Development (SPAD) 502 chlorophyll meter (Minolta corporation, Ltd., Osaka, Japan). The SPAD measures a unit less chlorophyll reflectance in the leaf using the Red and Infrared portions of the electromagnetic spectrum (Brewer et al., 2022). Finally, at the R6 phenological stage, marking the end of the growing season, the designated maize crops underwent sampling, involving cutting the aboveground foliage, followed by weighing it using a mass balance to determine the fresh AGB values at each sampling point. No mass correction was performed on the maize crops, considering their crucial role in small-scale farming systems as a source of both livestock fodder and human consumption. The decision to retain moisture in the maize aligns with its practical use for easy swallowing, addressing the specific needs of both animals and humans during this stage of maturity.

UAV platform and remotely sensed data acquisition

The digital multispectral images were collected over four phenological stages using a DJI Matrice 300 series (M300) UAV platform (SZ DJI Technology Co., Ltd, China) mounted with a MicaSense Altum multispectral and thermal sensor (AgEagle Aerial Systems Inc, Kansas) (Fig.2a). The Altum sensor is equipped with six spectral bands [red (668 nm), green (560 nm), blue (475 nm), red edge (717 nm), near-infrared (840), and thermal band (8 to 14 nm)] (Fig.2c). The M300 is equipped with Internet of Things (IoT) technology, such as obstacle avoidance sensors and a locational GPS connected to the camera, making the drone safe to operate and capture automatically georectified images. The UAV flights were conducted simultaneously with field measurements. A flight path covering the experimental field was digitized from Google Earth Pro and imported into the drone controller (Fig.2b). Before and after each flight, a whiteboard calibration panel was used to calibrate the reflectance of the images (Fig.2d). The calibration panel was used to determine illumination and atmospheric conditions during the flight for accurate vegetation indices retrieval. The flights were conducted between 10:00 a.m. and 14:00 p.m. under open sky and suitable weather conditions for optimum sunlight reflectance. The drone was operated at 15 m/s speed and 100 m altitude with 80% forward and 70% side overlap. The images were collected at 6 cm per pixel spatial resolution, based on 8mm focal length and 8° x37° field of view (FOV) angle.

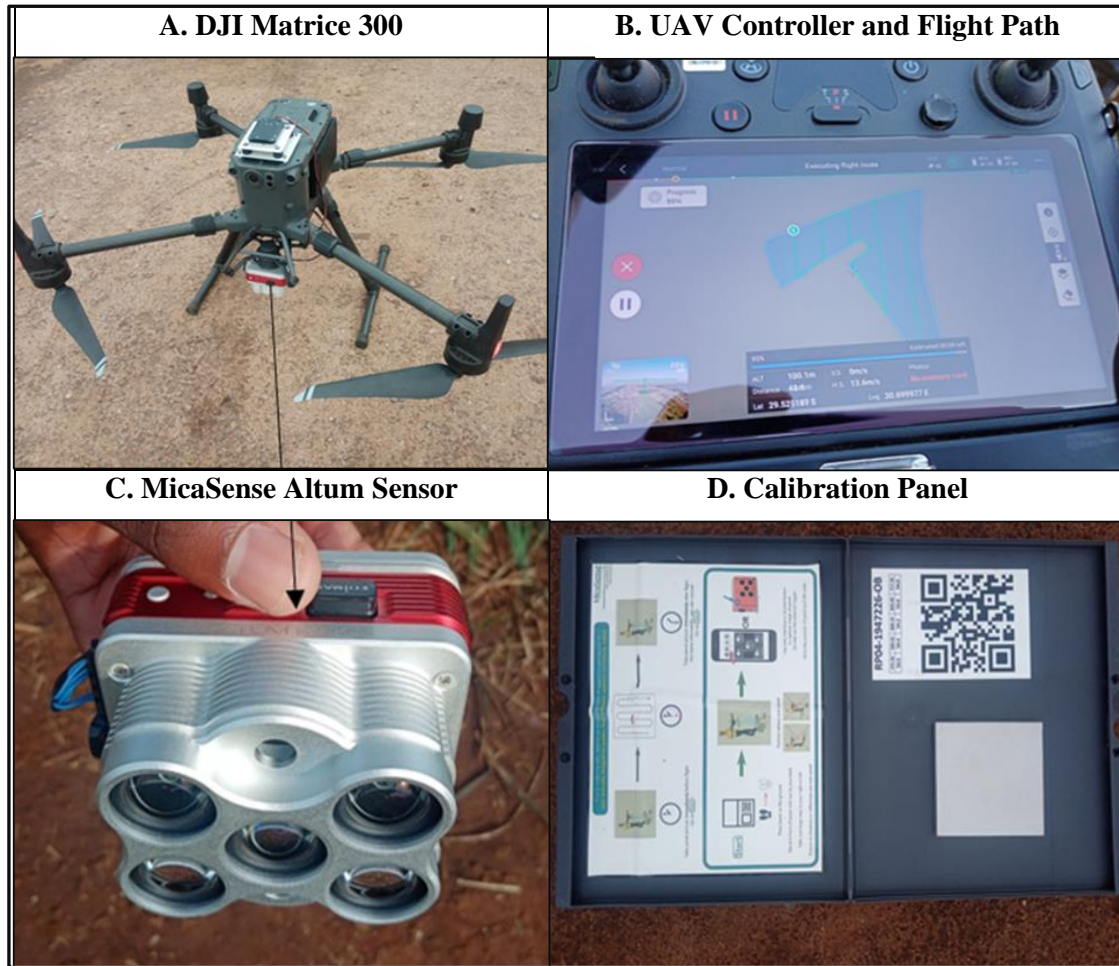


Figure 2. The UAV platform, controller with flight plan, image sensor, and calibration panel used for remotely sensed data acquisition in this study.

Image pre-processing and retrieval of vegetation indices

A total of 480 images were collected during each flight at each sampled growth stage. During the flights, the digital images were automatically georectified by the GPS payload mounted on the M300 UAV platform. Subsequently, the Pix4D 4.6 Fields photogrammetry software (Pix4D Inc. Denver, USA) was used to pre-process the images and generate an orthomosaic image and a digital elevation model (DEM). In addition, the index calculator of the Pix4D photogrammetry software was used to calculate optimal vegetation indices for estimating maize AGB (Table 2). The Pix4D index calculator uses mathematical equations from the Index Data Base (IDB) (<https://www.indexdatabase.de/>) to compute vegetation indices and provide a raster data showing their spatial distribution. The maize sample points, orthomosaic, and vegetation index raster images were imported into ArcGIS pro 10.7.1 software for data extraction using the ‘extract multi-values to points’ in the Arc Toolbox. The extracted band reflectance and vegetation indices for each sample point were then exported into Microsoft Excel for statistical analysis. Evidence from literature has proven the efficiency of vegetation indices in predicting maize AGB (Han et al., 2019b; Li et al., 2020; Li et al., 2016; Yue et al., 2023).

Table 2. Selected optimum vegetation indices for predicting maize AGB.

Vegetation Index	Formula	Reference
NDVI	$\frac{NIR - RED}{NIR + RED}$	(Shi & Xingguo, 2011)
CVI	$NIR \left(\frac{RED}{(GREEN)(GREEN)} \right)$	(Hunt Jr et al., 2011)
BNDVI	$\frac{NIR - BLUE}{NIR + BLUE}$	(Wang et al., 2007)
NDVI_Rededge	$\frac{Rededge - RED}{Rededge + RED}$	(Ehammer et al., 2010)
RBNDVI	$\frac{NIR - (RED + BLUE)}{NIR + (RED + BLUE)}$	(Wang et al., 2007)
ENDVI	$\frac{((NIR + GREEN) - (2 * BLUE))}{((NIR + GREEN) + (2 * BLUE))}$	(Ahamed et al., 2011)
CI_Rededge	$\frac{NIR}{Red - edge} - 1$	(Hunt Jr et al., 2011)
GLI	$\frac{2(GREEN - RED - BLUE)}{2(GREEN + RED + BLUE)}$	(Baroni et al., 2004)
EVI	$2.5 * \frac{(NIR - RED)}{(NIR + 6RED - 7.5BLUE) + 1}$	(Glenn et al., 2010)
EVI2	$2.4 * \frac{NIR - RED}{NIR + RED + 1}$	(Miura et al., 2008)
IPVI	$\frac{NIR}{\frac{NIR + RED}{2}}(NDVI + 1)$	(Kooistra et al., 2003)
SAVI	$\frac{NIR - RED}{NIR + RED + 0.5}(1 + 0.5)$	(Heiskanen, 2006)
OSAVI	$(1 + 0.16) \frac{NIR - RED}{NIR + RED + 0.16}$	(Wu et al., 2008)
SR	$\frac{NIR}{RED}$	(Malthus et al., 1993)
CI_Green	$\frac{NIR}{GREEN} - 1$	(Ahamed et al., 2011)
GDVI	$NIR - GREEN$	(Tucker et al., 1979)

Where, NDVI= Normalized Difference Vegetation Index, CVI= Chlorophyll Vegetation Index, BNDVI= Blue Normalized Difference Vegetation Index, NDVI_Rededge =Normalized Difference Vegetation Index Red edge, RBNDVI= Red Blue Normalized Difference Vegetation Index, ENDVI= Enhanced Normalized difference Vegetation Index, CI_Rededge= Chlorophyll Index Red edge, GLI= Green Leaf Index, EVI= Enhanced Vegetation Index, IPVI= Infrared Percentage Vegetation Index, SAVI= Soil Adjusted Vegetation Index, OSAVI= Optimised Soil Adjusted Vegetation Index, SR= Simple Ratio, CI_Green= Chlorophyll Index Green, GDVI= Generalised Difference Vegetation Index

Retrieval of landscape variables

To complete the objective of this study, landscape variables that significantly influence maize growth such as slope and aspect were acquired from the System for Automated Geoscientific Analyses (SAGA) Geographic Information Systems (GIS) 7.8.2 software (University of Hamburg, Germany). The digitized experimental field boundary and maize sample points were then used to clip and extract the landscape variables to the extent of the study area using ArcGIS Pro. Even though soil moisture was measured in-field together with biophysical variables, it was categorized under landscape variables because it quantifies the amount of water held by the soil. In addition, the DEM generated by Pix4D software was used to extract elevation data to the maize sample points as a landscape variable. The UAV remotely sensed data was then combined with the extracted landscape variables and field-measured biophysical variables in an Excel file for statistical analysis (Table 3). The data was then split into training (70%), and testing (30%) datasets using randomisation, thereby ensuring non-bias splitting and ensuring representative subsets for model training and validation.

Table 3. Input variables.

Variable	Data type	Number of variables
Remotely sensed	Spectral bands Vegetation indices	21
Landscape variables	Aspect Elevation Slope Soil moisture	4
Biophysical variables	Leaf chlorophyll content LAI	2
Total	8	27

AGB prediction

Deep learning architecture

Jupyter notebook extended from Anaconda3 was used to build a fully connected DNN model featuring 17 inputs, three hidden, and one output layer using python programming environment for predicting maize AGB at four phenological stages (Fig.3). The combination of innovative computational tools and sophisticated DNN architecture facilitates precise AGB predictions, contributing to a deeper understanding of maize growth dynamics and potential applications in agriculture (Coulibaly et al., 2022; Fuentes et al., 2017). DNN models are powerful in capturing non-linear relationships by self-learning from large datasets and make precise predictions (Zhang et al., 2022). DNN models use multiple layers with fully connected neurons that are similar to human brain neurons and known to produce highly accurate results, surpassing human experts (Saranya et al., 2023; Z. Zeng et al., 2022). Therefore, DNN have the potential to improve prediction accuracy of maize AGB compared to other traditional machine learning and statistical methods.

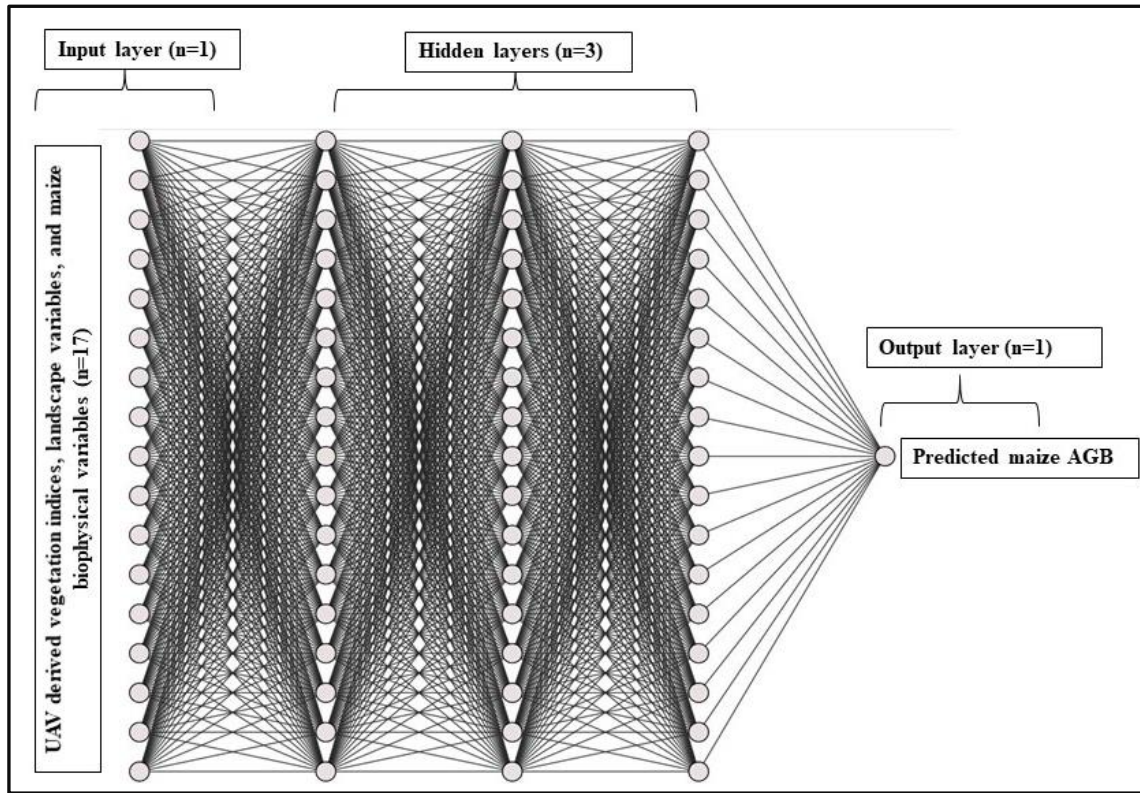


Figure 3. The diagrammatic illustration of the DNN model.

A good selection of hyperparameters based on the dataset is essential for building an optimum model (Dominguez-Olmedo, 2019). Therefore, the rectified linear unit (ReLU) was used in the input and hidden layers, respectively, to introduce non-linearity in the model. Linearity in DNN imply that all hidden layers have the same power in predicting the output (Kapočiūtė-Dzikiėnė et al., 2020). Due to the complexity and non-linearity within datasets, the hidden layers must have different magnitude of power in predicting the output (Tsai & Fang, 2021). Therefore, it is essential to introduce activation functions in the neural network to distinguish the hidden layers from each other for better detection and learning of the non-linear relationship between the input and predictor variables (Dubey et al., 2022; Jiang et al., 2022; X. Wang et al., 2022). The model was run over 500 epochs, implying that weights in the hidden layers were constantly adjusted five hundred times to minimize error and improve the maize AGB prediction accuracy. The input data is forwardly propagated to the hidden layers, where the weights and biases in the neurons predict the output by self-learning non-linear patterns from the input dataset. The loss functions quantify the deviation from the expected output and backwardly propagate the output to the hidden layers for adjustments in pursuit of minimising the prediction error (Dubey et al., 2022)

The output layer was fed with a SoftMax activation function and ‘Adam’ optimizer for model optimization and best results. Optimizers reduce the loss by selecting optimum weights in hidden layers to determine an optimum model for accurate prediction (Cho et al., 2020). Adam is known to surpass other optimizers such as stochastic gradient descent due to its ability of generalization and convergence speed within new datasets (Gaddam et al., 2022; Salem et al., 2022; Y. Wang et al., 2022). A batch size of 32 and normal initialization were also implemented in the model for best

results. Neural network models are well known for overfitting, which is explained as when the training dataset yields significantly better results than the testing dataset (Frei et al., 2022). Such model cannot be generalized and cannot accurately predict from an unknown dataset. Therefore, the L2 regularization (0.001) and a dropout of 0.4 were implemented in the layers of the model to minimise overfitting. The dropout and regularization features in DNN minimize loss between the predicted output and observed input and nullify the contribution of “bad” neurons towards subsequent layers, hence a better prediction accuracy.

Accuracy assessment

The Root Mean Square Error (RMSE) and coefficient of determination (R^2) were used to evaluate the metrics. The RMSE is the difference between the predicted and the observed output, while the R^2 reflects the percentage of the AGB variance that is explained by the model. The best performing model is represented by a higher R^2 value and a lower RMSE. The variable importance in predicting maize AGB was evaluated using the SHapley Additive exPlanations (SHAP) approach. The SHAP uses a theoretic approach that selects the top twenty variables of high magnitude impact in the performance of the model (Ekanayake et al., 2022).

Data preparation, variables selection, and model validation

Data preparation and variables selection

The correlation coefficient (R) was calculated between the predictor variables using correlation heat maps to choose significantly low correlated values for best results (Fig.4). Thereafter, highly correlated variables within the dataset were identified and removed to ensure maximum prediction accuracy as such variables have technically the same magnitude impact in the performance of the model.

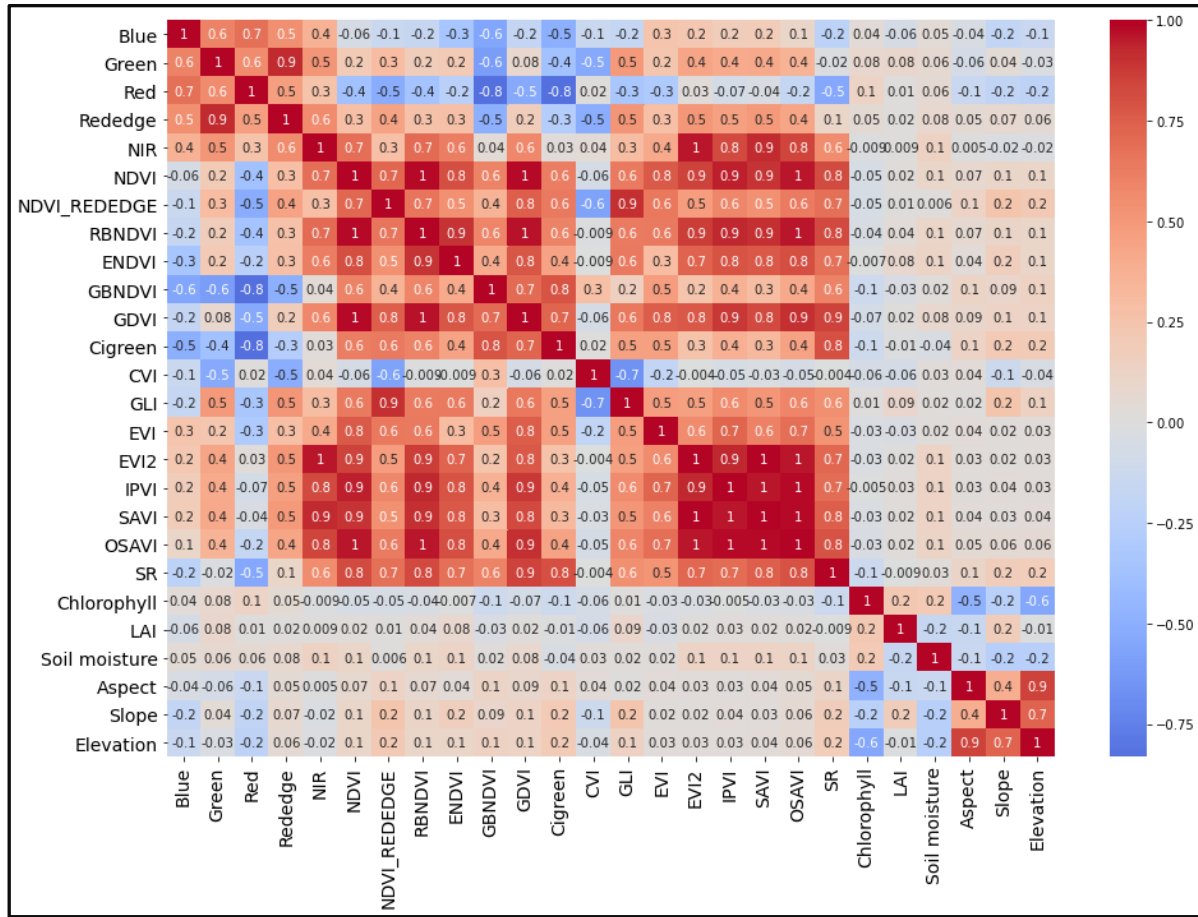


Figure 4. Pearson correlation (R) between the selected maize AGB predictor variables for all the phenological stages.

DNN model validation

Fig.5 shows loss curves during the validation of the DNN model using the training and test dataset over 500 epochs. Model validation is necessary for evaluating the performance of the DNN during self-learning from the dataset. The data was separated into 70% training and 30% testing dataset, and subsequently validated using the latter. The training and validation curves showed a uniform function, implying a gradual decrease in the maize AGB prediction error across all the phenological stages, hence the model was perfectly validated. An optimum model for predicting maize AGB was established and tested using the training dataset.

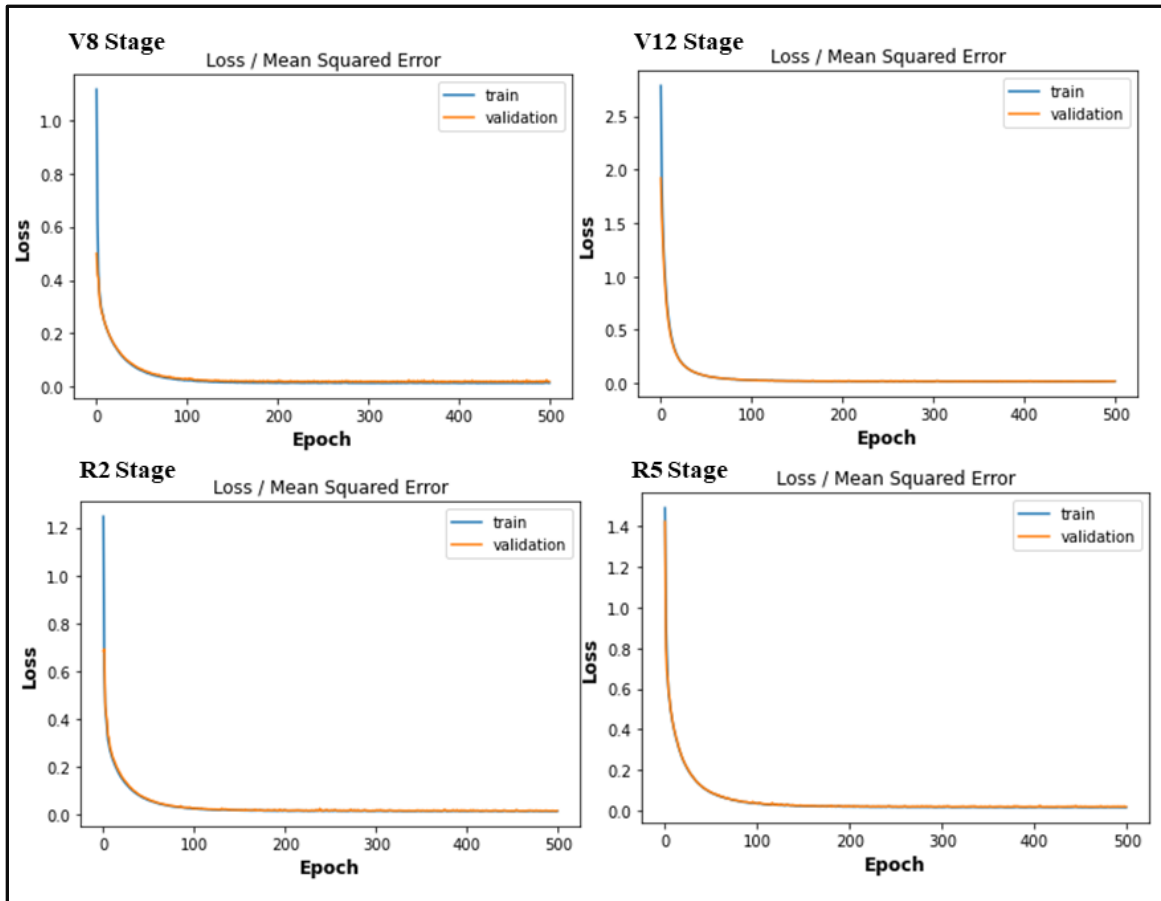


Figure 5. Loss graphs for model validation during all the phenological stages.

RESULTS

Descriptive statistics

The variations in field-measured biophysical and landscape variables of maize crops are shown in Table 4. On average, the recorded SPAD unit-less leaf chlorophyll content was 39.26, 37.38, 31.22, and 41.36 during the V8, V12, R2, and R5 phenological stages, respectively. The R5 phenological stage recorded the highest average chlorophyll content of 41.36. Soil moisture averages were 21.87%, 21.41%, 16.97%, and 19.1% during the V8, V12, R2, and R5 phenological stages, respectively. It was observed that soil moisture content decreased with growth from the V8-R5 phenological stages. The averages for LAI were 3.64, 2.78, 3.25, and 3.16 during the V8, V12, R2, and R5 phenological stages, respectively, with V8 recording the highest average.

Landscape variables are not subjected to rapid changes over a short time and were therefore assumed to be the same throughout the duration of the study. The average slope, elevation, and aspect were 9%, 856 m, and 2.73 degrees, respectively. The slope, elevation, and aspect ranged from 2% to 14%, 847m to 862m, and 2.20 degrees to 3.42 degrees, respectively. The recorded maize AGB was 1.19 kg/m² on average and ranged from 0.4 kg/m² to 1.81 kg/m², with 2.03 kg/m² and 2.11 kg/m² recorded as outliers. The outliers were due to measurement errors in the field and were therefore removed from the analysis for best results.

Table 4. Descriptive statistics of field measured biophysical and landscape variables across all phenological stages.

Field measured variables	V8 Stage				
		Range (Min-Max)	Mean	Median	Std.
	Chlorophyll	31.36-49.61	39.26	38.99	2.59
	LAI	13.99-27.01	21.87	22.16	2.21
	Soil Moisture (%)	2.48-4.64	3.64	3.64	0.25
	V12 Stage				
		Range (Min-Max)	Mean	Median	Std.
	Chlorophyll	29.70- 44.76	37.38	37.60	2.62
	LAI	15.67- 30.41	21.41	21.06	1.57
	Soil Moisture (%)	1.62- 4.58	2.78	2.74	0.23
	R2 Stage				
		Range (Min-Max)	Mean	Median	Std.
	Chlorophyll	21.36- 47.49	31.22	31.55	4.17
LAI	13.52- 23.67	16.97	16.64	1.36	
Soil Moisture (%)	1.92- 7.75	3.25	3.38	0.49	
R5 Stage					
	Range (Min-Max)	Mean	Median	Std.	
Chlorophyll	21.6-59.4	41.36	41.7	6.27	
LAI	10.6-31.3	19.68	19.4	4.13	
Soil Moisture (%)	1.41-6.8	3.16	3.03	4.85	
Landscape variables	Across all stages				
		Range (Min-Max)	Mean	Median	Std.
	Slope (%)	2-14	9	10	4
	Elevation (m)	847-862	856	857.6	4.02
	Aspect (degrees)	2.20-3.42	2.73	2.68	0.30

Deep Neural Network model evaluation in maize AGB prediction

Fig. 6 illustrates the maize AGB prediction results obtained when the most important and best performing variables were combined for all phenological stages. The V8 ($R^2=0.65$, $RMSE= 0.1 \text{ kg/m}^2$, $RMSE\%=8.5\%$) and R5 ($R^2=0.67$, $RMSE= 0.091 \text{ kg/m}^2$, $RMSE\%=7.6\%$) phenological stages had a relatively lower prediction accuracy. However, the prediction error was within the 10 % accepted range. The V12 ($R^2=0.74$, $RMSE=0.07 \text{ kg/m}^2$, $RMSE\%=5.9\%$) and R2 ($R^2=0.71$, $RMSE=0.086 \text{ kg/m}^2$, $RMSE\%=7.3\%$) phenological stages performed optimally, with relatively high prediction accuracy.

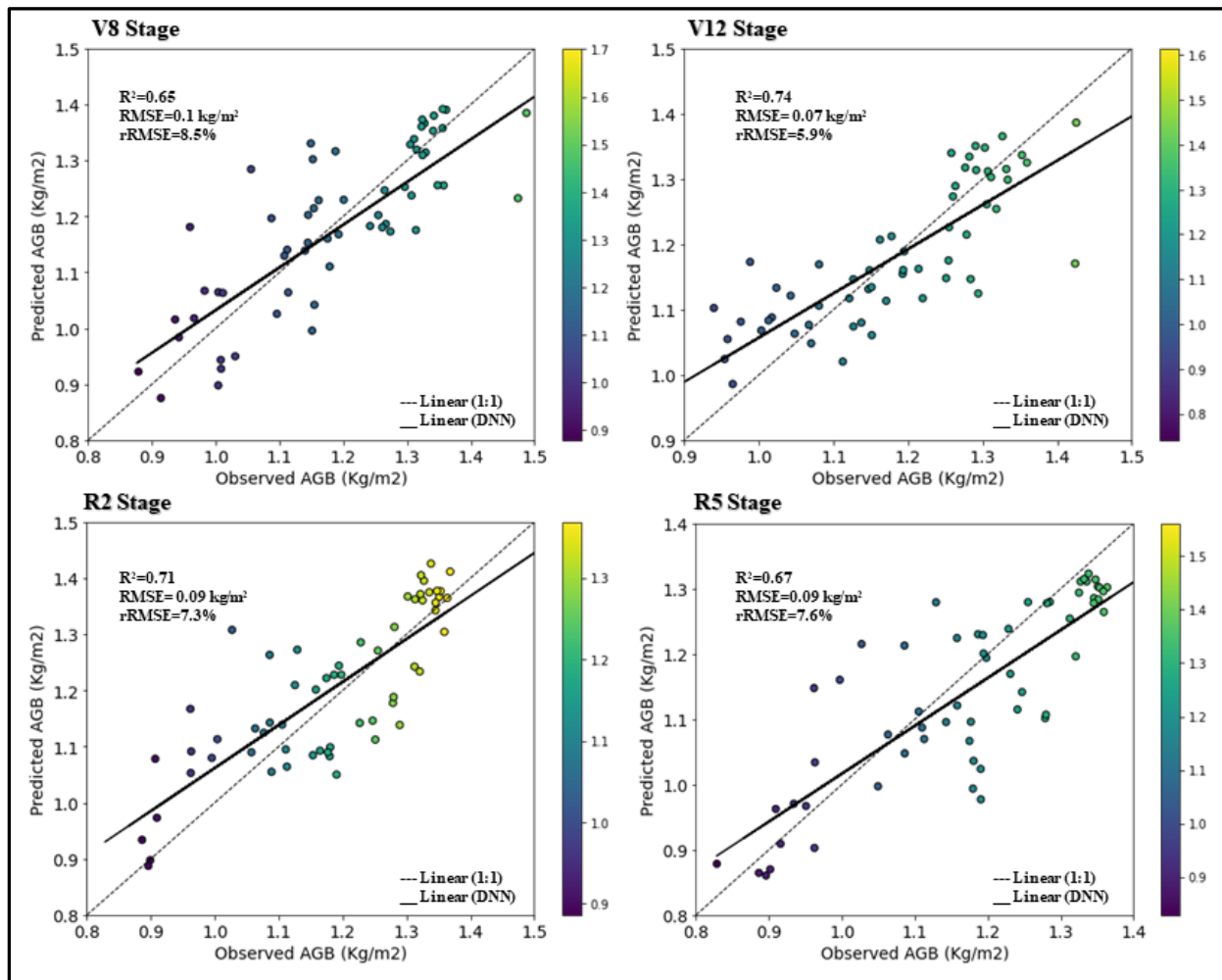


Figure 6. Predicted maize AGB using DNN model for the V8, V12, R2, and R5 phenological stages.

Variable importance assessment

Fig. 7 shows the most important variables in the prediction of maize AGB by the DNN model using the SHAP approach. The SR vegetation index was most important during the V8 and R2, while leaf chlorophyll content and elevation were most influential during the V12 and R5 phenological stages. The figure shows that all landscape variables were important in the prediction of maize AGB across all phenological stages. The biophysical variables (LAI and leaf chlorophyll content) were among the top six important variables during the V8, V12, and R5 phenological stages, while the Red spectral band was the least important variable in maize AGB prediction across all phenological stages. EVI had an extremely low importance in predicting maize AGB during the V12 and R5 phenological stages.

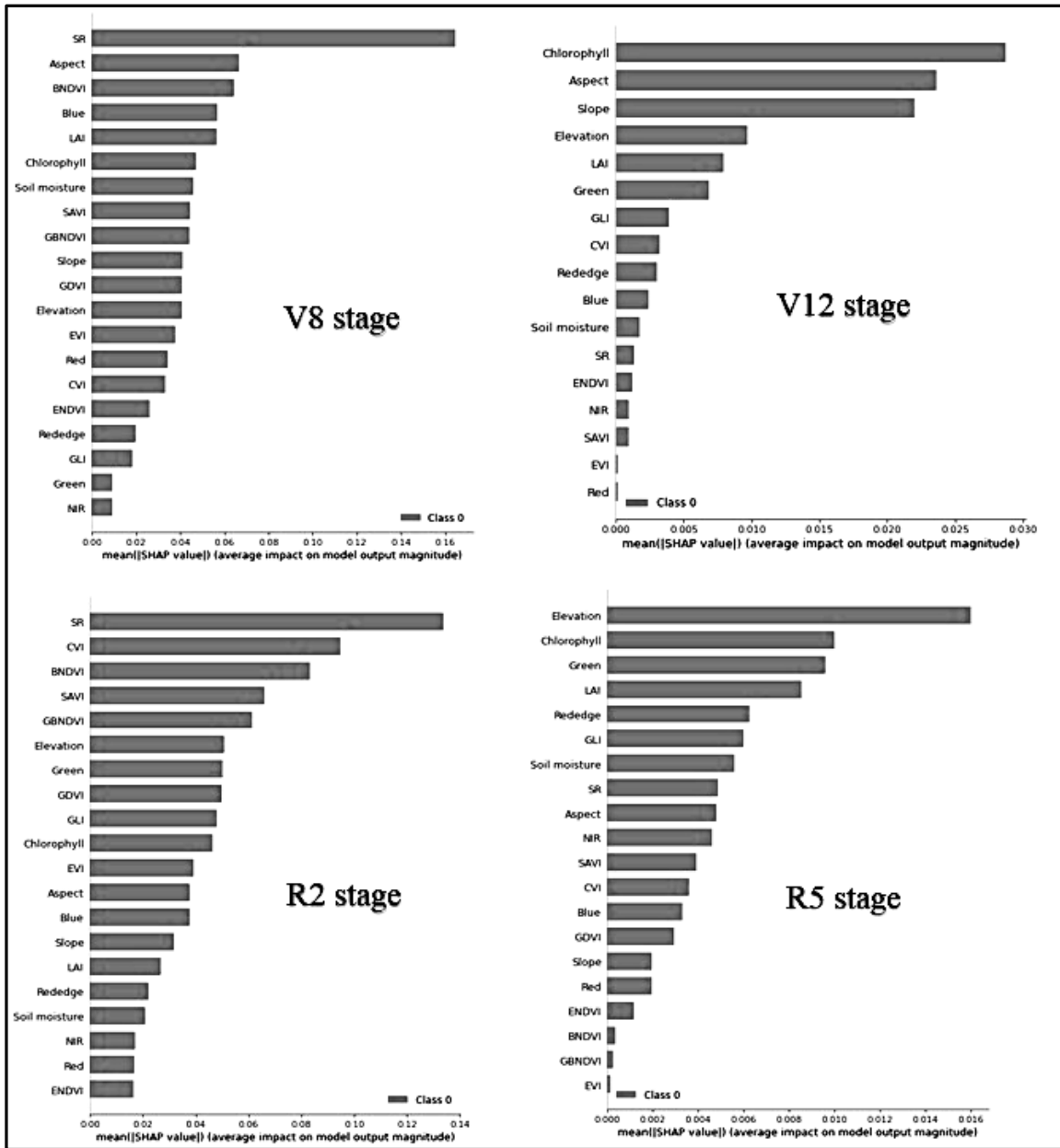


Figure 7. SHAP generated variable importance ranking of the model’s input variables for all the phenological stages.

Mapping the spatial distribution of predicted AGB across the phenological stages

Fig.8 shows the spatial distribution of predicted maize AGB during all the phenological stages. The spatial distribution map was generated utilizing the important predictor variables (Fig.7) for maize AGB prediction and the equation of the line of best fit derived from scatter plots comparing predicted and observed AGB at each phenological stage. Typically, a raster file of the most important maize AGB predictor variable is generated using ArcMap, and the equation $y=mx+c$ is applied, substituting x with the raster file. The generated distribution maps show an increase in maize AGB from the V8 to the R2 phenological stage. There was a slight decrease in the concentration of AGB during the R5 stage. This distribution is also shown by the prediction

accuracy previously presented in Fig.6, which shows relatively higher prediction accuracy during the V8 and the R1, and lower during the R5 and V8 phenological stages. Similarly, the distribution maps show the same relationship in maize AGB concentration. During all phenological stages, high AGB concentration was observed towards the edges and the field's downslope. In addition, during all the phenological stages, low AGB was observed in a middle of the experimental field.

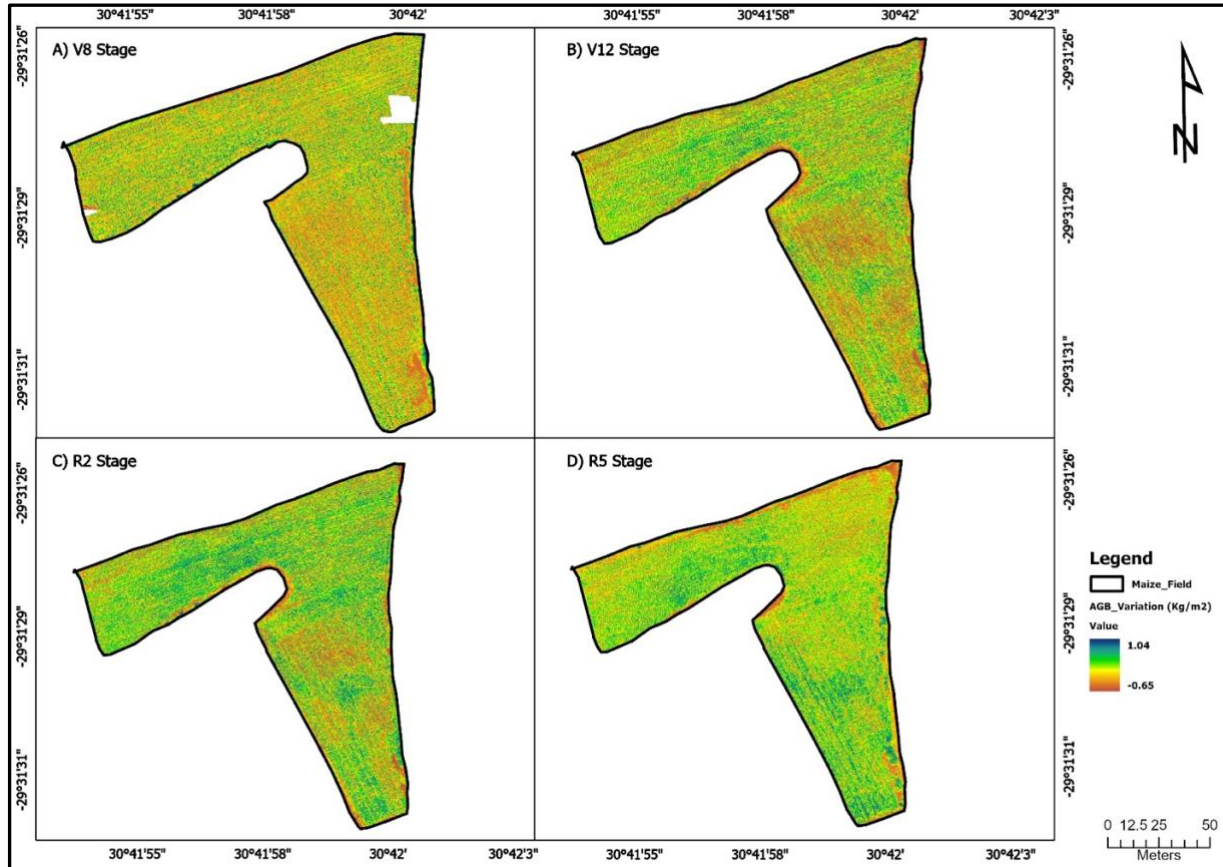


Figure 8. Spatial distribution of predicted maize AGB across all the phenological stage.

DISCUSSION

In developing countries, small-scale farming systems typically lack crop monitoring resources and knowledge on techniques to optimize yield (Onyango et al., 2021). Hence, this study bridged the gap by implementing an affordable crop monitoring resources such as the in-situ instruments, the UAV platform and sensor to accurately estimate maize AGB, which can serve as a proxy to yield. Specifically, this study aimed to develop a model that can accurately predict maize AGB and determine the optimal phenological stage for maize AGB estimation.

The potential of UAV-remotely sensed data in predicting maize AGB

Unmanned Aerial Vehicle-remotely sensed data offer a promising capability to effectively estimate maize AGB in small spatial extents. This is attributed to the remarkable ability of the platform mounted with sophisticated sensors to provide high spatial resolution dataset, enabling individual

sensing and assessment of maize crops for accurate AGB estimation (Khun et al., 2021; Niu et al., 2019). Unmanned Aerial Vehicle-mounted cameras such as multispectral sensors offer a broad range of the electromagnetic bands including the visible, NIR, Red-edge, and thermal sections, allowing for efficient retrieval of vegetation indices capable of estimating maize AGB (Olson & Anderson, 2021). This study successfully predicted AGB at various maize phenological stages using UAV-remotely sensed data and deep learning approach. The results indicated that the V12 and R2 phenological stage reported relatively high accuracy in AGB predictions ($R^2=0.74$ and $RMSE=0.07 \text{ kg/m}^2$) and ($R^2=0.71$ and $RMSE= 0.086 \text{ kg/m}^2$), respectively. The V12-R2 phenological stages are the mid-stages of maize growth cycle and portray dark green leaves, symbolizing a high concentration of leaf chlorophyll content (Herrmann et al., 2010). Hence, the best results were obtained during the V12-R2 period due to optimum reflectance of maize leaves and minimal soil background noise. The findings of our study concur with B. Yang et al. (2022) who used multi-temporal and mono-temporal UAV-remotely sensed data and noted that R3 was the most suitable phenological stage for maize AGB prediction. Similarly, Amanullah et al. (2009) investigated maize yield using traditional methods, and established that the V12-R1 phenological stages had relatively higher yield compared to other phenological stages. Therefore, based on our results, we can deduce that V12-R2 is the optimum phenological stage for maize AGB estimation.

The V8 phenological stage and R5 phenological stages had lower maize AGB prediction accuracies, i.e., $R^2 = 0.65$ and $R^2 = 0.67$, respectively. This was because the maize canopy was not fully developed and soil background was more pronounced at V8 stage, hence, interfering with maize reflectance signatures (Y. Zeng et al., 2022). The spatial distribution map shows a high maize AGB downslope and some parts of the field where soils were thick and appeared rich in nutrients (Fig.8). Thin soils were also observed upslope and in some parts of the field; low maize AGB was observed in those areas. Considering that the study area is small, there was a significant variation in soil thickness, which is why the predicted concentration of maize AGB is not uniform across the experimental field. Thick soils have a better water retention and nutrient holding capacity for crop's use, hence higher maize AGB (Mu et al., 2018).

Brewer et al. (2022) noted that NIR derived vegetation indices can surpass variable background effects compared to conventional bands. The soil-adjusted vegetation indices were selected to eliminate soil background and accurately predict maize AGB. As expected, SAVI was among the significantly influential variables in the estimation of maize AGB during all the phenological stages, including the V8 where vegetation cover was minimal. The R5 phenological stage was characterized by dry-denting leaves and marked the end of mass gain. We speculate that the dry leaves significantly reduced the reflectance; hence remotely sensed variables were less important and lower maize AGB prediction accuracy was observed during this stage. While Red-edge-based vegetation indices were influential, they did not have a significant contribution to AGB prediction as compared to NIR-derived indices. The findings of this study are supported by Gao et al. (2017) who confirmed the efficacy of vegetation index-based biomass estimation in maize crops.

Plant biophysical variables in maize AGB prediction

The relationship between LAI, leaf chlorophyll content, and AGB is crucial in understanding the physiological and agronomic aspects of maize growth and productivity (Ban et al., 2019). LAI represents the total leaf area per unit ground area and is often indicates the canopy structure and the light interception capacity of maize crop (Liu et al., 2022). It is positively correlated with photosynthetic activity, as a higher LAI generally implies a larger surface area for light absorption,

hence high productivity (Li et al., 2023). Leaf chlorophyll content is a key factor influencing photosynthesis, as chlorophyll is responsible for capturing light energy and transform it into chemical energy (Y. Guo et al., 2020). Higher chlorophyll content is generally associated with increased photosynthetic rates, contributing to greater biomass production (Meena et al., 2021). Hence, optimal LAI and chlorophyll content contribute to enhanced photosynthesis, leading to increased biomass accumulation in maize crops.

In this study, the recorded leaf chlorophyll content was higher in the early stage (V8) and the late reproductive stage (R5). This is supported by Brewer et al. (2022) who noted that high chlorophyll concentrations are associated with early vegetation and late reproduction stages when maize grows rapidly and kernelling, respectively. Similarly, leaf chlorophyll content in the early and late reproductive stages is associated with high LAI (H. Yang et al., 2022). As shown by the SHAP variable importance approach, leaf chlorophyll content had a relatively high impact on maize AGB prediction across all the phenological stages. Our results concur with Liu et al. (2019) who established a positive co-relationship between maize AGB and leaf chlorophyll content. In addition, LAI also had a relatively high impact on maize AGB prediction during the V8, V12, and R5 phenological stages. Contrary to our results, Tang et al. (2023) also established a strong relationship between LAI and maize yield after the R1 phenological stage in maize crops.

The potential of landscape variables on improving maize AGB prediction

Landscape variables significantly increased the maize AGB prediction accuracy and were all important during all the phenological stages (Fig.7). In addition, the landscape variables were less correlated to each other, hence the DNN model performed well with their inclusion. A study by Sun et al. (2023) successfully combined topographic variables and vegetation and texture indices to predict maize yield and obtained satisfactory results ($R^2 = 0.81$, RMSE = 0.297t/ha), which confirms the value of landscape variables in maize AGB prediction. Similarly, Behera et al. (2023) used elevation, slope, and aspect to model maize AGB, and obtained satisfactory results ($R^2 = 0.72$ and RMSE= 69.18 mg/ha). Salinas-Melgoza et al. (2018) modelled a relationship between landscape variables and noted that landscape variables explained 21% of AGB in reforested areas. Salinas-Melgoza et al. (2018) argued that human activities such as deforestation, land degradation, improper irrigation methods, changing land uses, and pollution have a significant impact on landscape alteration, while crops productivity heavily depend on landscape variables. These human activities facilitate soil erosion, urban expansion, and alterations of soil productivity which significantly affect the slope, aspect, elevation and soil water holding capacity (Mariye et al., 2022).

The performance of deep neural network model in maize AGB prediction

The deep learning approach in maize yield prediction was evaluated using UAV-remotely sensed data combined with biophysical and landscape variables. Furthermore, with DNN requirements for large datasets, the three variables used in this model were adequate to feed enough information to the model for accurate maize AGB prediction. The main objective of this study was to evaluate deep learning approach in maize AGB prediction, particularly with minimal dataset obtained from small spatial extent. To obtain a reliable statistical relationship, DNN require large sample size to effectively learn and discover patterns between the predictor and test variables (Zhang et al., 2021). Therefore, we sampled 200 points to generate an effective model. Based on the overall RMSE and RMSE% achieved in this study, our model had minimal prediction errors (< 10%) across all the phenological stages. In addition, combining three different sources of datasets improved the prediction accuracy of maize AGB. This was because DNN require a lot of complex and nonlinear

datasets to perform effectively. Han et al. (2019a) successfully modelled maize AGB in commercial farming systems using DNN and other machine learning algorithms and achieved satisfactory results. However, this study argues that DNNs require significant repeat training, necessitating a lot of computational power to obtain an optimal model in minimal time.

Implications and recommendations

Unmanned Aerial Vehicle-mounted multispectral sensors provide high resolution dataset, allowing for detection of crop agronomical characteristics facilitating maize AGB estimation (Zhai et al., 2023). However, the spectral information of crops remains coarse due to multispectral wide bands portraying lower spectral resolution. Therefore, hyperspectral remote sensing for precise spectral information retrieval and effective maize AGB prediction is highly recommended. Additionally, the study concluded that landscape variables have a significant impact on maize AGB prediction. However, the analysis did not include an assessment of the magnitude of each landscape variable's influence on maize AGB prediction. Hence, it is recommended that forthcoming research endeavours explore the specific impact of individual landscape variables in the prediction of maize AGB. This will contribute to the improvement of validated data availability for further yield predictions. The DNN model requires extensive hyperparameters adjustments to obtain an optimal model. Consequently, its suitability for tasks demanding rapid turnaround times is not recommended. The acquired DNN model was trained using maize derived datasets, and validated using unknown maize dataset, thereby enhancing its applicability in other locations with variability in landscape variables. However, the performance of the acquired model remains limited to adequate dataset and applicable to maize AGB prediction only. Despite the success of the DNN model in adequately predicting maize AGB, more studies need to extensively explore the full potential of this approach, considering its promising potential to make accurate predictions. Despite the success of the DNN model in adequately predicting maize AGB, more studies need to extensively explore the full potential of this approach, considering its promising potential to make accurate predictions.

CONCLUSION

The study sought to assess the utility of landscape and biophysical variables combined with UAV-remotely sensed data in predicting maize AGB using the DNN algorithm at four phenological stages (V8, V12, R2, and R5). Based on the attained results, it can be concluded that:

- The V12-R1 phenological stages are optimal for maize AGB prediction when vegetation reflectance is at peak.
- Landscape variables improve the prediction accuracy of maize AGB and can therefore be used in maize AGB estimation.
- The Near infrared spectral bands were the most influential variables in predicting maize AGB prediction.
- Landscape variables, biophysical variables, and UAV-remotely sensed vegetation indices demonstrated significant importance in predicting maize AGB. Hence, the combination of these variables has demonstrated the ability to improve maize AGB prediction, underscoring the effectiveness achieved through their collaborative utilization in this study.
- Finally, the DNN algorithm yielded satisfactory results, attributable to the combined dynamic and non-linear datasets in pursuit of a good model.

The results of this study have a significant contribution to precision agriculture particularly in underprivileged small-scale farming systems. Furthermore, the findings of this study address gaps in the current literature, notably by introducing smart agriculture concepts to the global south for improved maize production and sustenance.

REFERENCES

- Aasen, H., Honkavaara, E., Lucieer, A., & Zarco-Tejada, P. J. (2018). Quantitative remote sensing at ultra-high resolution with UAV spectroscopy: a review of sensor technology, measurement procedures, and data correction workflows. *Remote sensing*, 10(7), 1091.
- Adewopo, J., Peter, H., Mohammed, I., Kamara, A., Craufurd, P., & Vanlauwe, B. (2020). Can a combination of uav-derived vegetation indices with biophysical variables improve yield variability assessment in smallholder farms? [Article]. *Agronomy*, 10(12), Article 1934. <https://doi.org/10.3390/agronomy10121934>
- Ahamed, T., Tian, L., Zhang, Y., & Ting, K. (2011). A review of remote sensing methods for biomass feedstock production. *Biomass and bioenergy*, 35(7), 2455-2469.
- Ali, A. M., Abouelghar, M., Belal, A., Saleh, N., Yones, M., Selim, A. I., Amin, M. E., Elwesemy, A., Kucher, D. E., & Maginan, S. (2022). Crop yield prediction using multi sensors remote sensing. *The Egyptian Journal of Remote Sensing and Space Science*, 25(3), 711-716.
- Altaweel, M., Khelifi, A., Li, Z., Squitieri, A., Basmaji, T., & Ghazal, M. (2022). Automated archaeological feature detection using deep learning on optical UAV imagery: Preliminary results. *Remote sensing*, 14(3), 553.
- Amanullah, Yasir, M., Khalil, S. K., Jan, M. T., & Khan, A. Z. (2009). Phenology, growth, and grain yield of maize as influenced by foliar applied urea at different growth stages. *Journal of Plant Nutrition*, 33(1), 71-79.
- Ban, H.-Y., Ahn, J.-B., & Lee, B.-W. (2019). Assimilating MODIS data-derived minimum input data set and water stress factors into CERES-Maize model improves regional corn yield predictions. *PLoS One*, 14(2), e0211874.
- Baroni, F., Boscagli, A., Di Lella, L., Protano, G., & Riccobono, F. (2004). Arsenic in soil and vegetation of contaminated areas in southern Tuscany (Italy). *Journal of Geochemical Exploration*, 81(1-3), 1-14.
- Battude, M., Al Bitar, A., Morin, D., Cros, J., Huc, M., Sicre, C. M., Le Dantec, V., & Demarez, V. (2016). Estimating maize biomass and yield over large areas using high spatial and temporal resolution Sentinel-2 like remote sensing data. *Remote Sensing of Environment*, 184, 668-681.
- Behera, D., Kumar, V. A., Rao, J. P., Padal, S., Ayyappan, N., & Reddy, C. S. (2023). Estimating Aboveground Biomass of a Regional Forest Landscape by Integrating Textural and Spectral Variables of Sentinel-2 Along with Ancillary Data. *Journal of the Indian Society of Remote Sensing*, 1-13.
- Brewer, K., Clulow, A., Sibanda, M., Gokool, S., Naiken, V., & Mabhaudhi, T. (2022). Predicting the chlorophyll content of maize over phenotyping as a proxy for crop health in smallholder farming systems. *Remote sensing*, 14(3), 518.
- Buthelezi, S., Mutanga, O., Sibanda, M., Odindi, J., Clulow, A. D., Chimonyo, V. G., & Mabhaudhi, T. (2023). Assessing the prospects of remote sensing maize leaf area index using UAV-derived multi-spectral data in smallholder farms across the growing season. *Remote sensing*, 15(6), 1597.

- Cao, Y., Chen, Z., Belkin, M., & Gu, Q. (2022). Benign overfitting in two-layer convolutional neural networks. *Advances in neural information processing systems*, 35, 25237-25250.
- Che, Y., Wang, Q., Zhou, L., Wang, X., Li, B., & Ma, Y. (2022). The effect of growth stage and plant counting accuracy of maize inbred lines on LAI and biomass prediction. *Precision Agriculture*, 23(6), 2159-2185.
- Cheng, M., Jiao, X., Liu, Y., Shao, M., Yu, X., Bai, Y., Wang, Z., Wang, S., Tuohuti, N., & Liu, S. (2022). Estimation of soil moisture content under high maize canopy coverage from UAV multimodal data and machine learning. *Agricultural Water Management*, 264, 107530.
- Cheng, Z., Meng, J., Ji, F., Wang, Y., Fang, H., & Yu, L. (2020). Aboveground biomass estimation of late-stage maize based on the WOFOST model and UAV observations [Article]. *Yaogan Xuebao/Journal of Remote Sensing*, 24(11), 1403-1418. <https://doi.org/10.11834/jrs.20200069>
- Cho, H., Kim, Y., Lee, E., Choi, D., Lee, Y., & Rhee, W. (2020). Basic enhancement strategies when using Bayesian optimization for hyperparameter tuning of deep neural networks. *IEEE access*, 8, 52588-52608.
- Coulibaly, S., Kamsu-Foguem, B., Kamissoko, D., & Traore, D. (2022). Deep learning for precision agriculture: A bibliometric analysis. *Intelligent Systems with Applications*, 16, 200102.
- Dominguez-Olmedo, R. (2019). Sample-Efficient Deep Reinforcement Learning for On-The-Fly Thermal Process Control in Laser Powder Bed Fusion University of Sheffield].
- Dubey, S. R., Singh, S. K., & Chaudhuri, B. B. (2022). Activation functions in deep learning: A comprehensive survey and benchmark. *Neurocomputing*.
- Ehammer, A., Fritsch, S., Conrad, C., Lamers, J., & Dech, S. (2010). Statistical derivation of fPAR and LAI for irrigated cotton and rice in arid Uzbekistan by combining multi-temporal RapidEye data and ground measurements. *Remote Sensing for Agriculture, Ecosystems, and Hydrology XII*,
- Ekanayake, I., Meddage, D., & Rathnayake, U. (2022). A novel approach to explain the black-box nature of machine learning in compressive strength predictions of concrete using Shapley additive explanations (SHAP). *Case Studies in Construction Materials*, 16, e01059.
- Frei, S., Chatterji, N. S., & Bartlett, P. (2022). Benign overfitting without linearity: Neural network classifiers trained by gradient descent for noisy linear data. *Conference on Learning Theory*,
- Fry, J. E., & Guber, A. K. (2020). Temporal stability of field-scale patterns in soil water content across topographically diverse agricultural landscapes. *Journal of Hydrology*, 580, 124260.
- Fuentes, A., Yoon, S., Kim, S. C., & Park, D. S. (2017). A robust deep-learning-based detector for real-time tomato plant diseases and pests recognition. *Sensors*, 17(9), 2022.
- Gaddam, D. K. R., Ansari, M. D., Vuppala, S., Gunjan, V. K., & Sati, M. M. (2022). A performance comparison of optimization algorithms on a generated dataset. *ICDSMLA 2020: Proceedings of the 2nd International Conference on Data Science, Machine Learning and Applications*,
- Gao, Y., Gao, J., Wang, J., Wang, S., Li, Q., Zhai, S., & Zhou, Y. (2017). Estimating the biomass of unevenly distributed aquatic vegetation in a lake using the normalized water-adjusted vegetation index and scale transformation method. *Science of the Total Environment*, 601, 998-1007.
- Gargiulo, J. I., Lyons, N. A., Masia, F., Beale, P., Insua, J. R., Correa-Luna, M., & Garcia, S. C. (2023). Comparison of Ground-Based, Unmanned Aerial Vehicles and Satellite Remote Sensing Technologies for Monitoring Pasture Biomass on Dairy Farms. *Remote sensing*, 15(11), 2752.

- Geng, L., Che, T., Ma, M., Tan, J., & Wang, H. (2021). Corn biomass estimation by integrating remote sensing and long-term observation data based on machine learning techniques. *Remote sensing*, 13(12), 2352.
- Gerke, D. (2019). An Evaluation of Unmanned Aerial Systems and Structure-From-Motion for Fluvial Large Wood Sensing and Risk Assessment.
- Glenn, E. P., Nagler, P. L., & Huete, A. R. (2010). Vegetation index methods for estimating evapotranspiration by remote sensing. *Surveys in Geophysics*, 31, 531-555.
- Goldenberg, M. G., Burian, A., Seppelt, R., Ossa, F. A. S., Bagnato, C. E., Satorre, E. H., Martini, G. D., & Garibaldi, L. A. (2022). Effects of natural habitat composition and configuration, environment and agricultural input on soybean and maize yields in Argentina. *Agriculture, Ecosystems & Environment*, 339, 108133.
- Guo, Y., Wang, H., Wu, Z., Wang, S., Sun, H., Senthilnath, J., Wang, J., Bryant, C. R., & Fu, Y. (2020). Modified red blue vegetation index for chlorophyll estimation and yield prediction of maize from visible images captured by uav [Article]. *Sensors (Switzerland)*, 20(18), 1-16, Article 5055. <https://doi.org/10.3390/s20185055>
- Guo, Y., Wang, H., Wu, Z., Wang, S., Sun, H., Senthilnath, J., Wang, J., Robin Bryant, C., & Fu, Y. (2020). Modified red blue vegetation index for chlorophyll estimation and yield prediction of maize from visible images captured by UAV. *Sensors*, 20(18), 5055.
- Haarhoff, S. J., Kotzé, T. N., & Swanepoel, P. A. (2020). A prospectus for sustainability of rainfed maize production systems in South Africa. *Crop Science*, 60(1), 14-28.
- Han, L., Yang, G., Dai, H., Xu, B., Yang, H., Feng, H., Li, Z., & Yang, X. (2019a). Modeling maize above-ground biomass based on machine learning approaches using UAV remote-sensing data. *Plant Methods*, 15(1), 10. <https://doi.org/10.1186/s13007-019-0394-z>
- Han, L., Yang, G., Dai, H., Xu, B., Yang, H., Feng, H., Li, Z., & Yang, X. (2019b). Modeling maize above-ground biomass based on machine learning approaches using UAV remote-sensing data. *Plant methods*, 15(1), 1-19.
- Heiskanen, J. (2006). Estimating aboveground tree biomass and leaf area index in a mountain birch forest using ASTER satellite data. *International Journal of Remote Sensing*, 27(6), 1135-1158.
- Herrmann, I., Karnieli, A., Bonfil, D., Cohen, Y., & Alchanatis, V. (2010). SWIR-based spectral indices for assessing nitrogen content in potato fields. *International Journal of Remote Sensing*, 31(19), 5127-5143.
- Hunt Jr, E. R., Daughtry, C., Eitel, J. U., & Long, D. S. (2011). Remote sensing leaf chlorophyll content using a visible band index. *Agronomy Journal*, 103(4), 1090-1099.
- Jiang, F., Sun, H., Ma, K., Fu, L., & Tang, J. (2022). Improving aboveground biomass estimation of natural forests on the Tibetan Plateau using spaceborne LiDAR and machine learning algorithms. *Ecological Indicators*, 143, 109365.
- Kapočiūtė-Dzikienė, J., Balodis, K., & Skadiņš, R. (2020). Intent detection problem solving via automatic DNN hyperparameter optimization. *Applied Sciences*, 10(21), 7426.
- Kayad, A., Sozzi, M., Gatto, S., Marinello, F., & Pirotti, F. (2019). Monitoring within-field variability of corn yield using Sentinel-2 and machine learning techniques. *Remote sensing*, 11(23), 2873.
- Khaki, S., & Wang, L. (2019). Crop yield prediction using deep neural networks. *Frontiers in plant science*, 10, 621.
- Khan, S. N., Li, D., & Maimaitijiang, M. (2022). A Geographically Weighted Random Forest Approach to Predict Corn Yield in the US Corn Belt. *Remote sensing*, 14(12), 2843.

- Khun, K., Tremblay, N., Panneton, B., Vigneault, P., Lord, E., Cavayas, F., & Codjia, C. (2021). Use of oblique RGB imagery and apparent surface area of plants for early estimation of above-ground corn biomass [Article]. *Remote Sensing*, 13(20), Article 4032. <https://doi.org/10.3390/rs13204032>
- Kooistra, L., Leuven, R., Wehrens, R., Nienhuis, P., & Buydens, L. (2003). A comparison of methods to relate grass reflectance to soil metal contamination. *International Journal of Remote Sensing*, 24(24), 4995-5010.
- Leroux, L., Castets, M., Baron, C., Escorihuela, M.-J., Bégué, A., & Seen, D. L. (2019). Maize yield estimation in West Africa from crop process-induced combinations of multi-domain remote sensing indices. *European Journal of Agronomy*, 108, 11-26.
- Li, B., Xu, X., Zhang, L., Han, J., Bian, C., Li, G., Liu, J., & Jin, L. (2020). Above-ground biomass estimation and yield prediction in potato by using UAV-based RGB and hyperspectral imaging. *ISPRS Journal of Photogrammetry and Remote Sensing*, 162, 161-172.
- Li, F., Hao, D., Zhu, Q., Yuan, K., Braghieri, R. K., He, L., Luo, X., Wei, S., Riley, W. J., & Zeng, Y. (2023). Vegetation clumping modulates global photosynthesis through adjusting canopy light environment. *Global Change Biology*, 29(3), 731-746.
- Li, W., Niu, Z., Chen, H., Li, D., Wu, M., & Zhao, W. (2016). Remote estimation of canopy height and aboveground biomass of maize using high-resolution stereo images from a low-cost unmanned aerial vehicle system. *Ecological Indicators*, 67, 637-648.
- Li, X., Geng, H., Zhang, L., Peng, S., Xin, Q., Huang, J., Li, X., Liu, S., & Wang, Y. (2022). Improving maize yield prediction at the county level from 2002 to 2015 in China using a novel deep learning approach. *Computers and Electronics in Agriculture*, 202, 107356.
- Li, Z., Zhao, Y., Taylor, J., Gaulton, R., Jin, X., Song, X., Li, Z., Meng, Y., Chen, P., & Feng, H. (2022). Comparison and transferability of thermal, temporal and phenological-based in-season predictions of above-ground biomass in wheat crops from proximal crop reflectance data. *Remote Sensing of Environment*, 273, 112967.
- Lischeid, G., Webber, H., Sommer, M., Nendel, C., & Ewert, F. (2022). Machine learning in crop yield modelling: A powerful tool, but no surrogate for science. *Agricultural and Forest Meteorology*, 312, 108698.
- Liu, C., Liu, Y., Lu, Y., Liao, Y., Nie, J., Yuan, X., & Chen, F. (2019). Use of a leaf chlorophyll content index to improve the prediction of above-ground biomass and productivity. *PeerJ*, 6, e6240.
- Liu, G., Yang, Y., Liu, W., Guo, X., Xie, R., Ming, B., Xue, J., Zhang, G., Li, R., & Wang, K. (2022). Optimized canopy structure improves maize grain yield and resource use efficiency. *Food and Energy Security*, 11(2), e375.
- Liu, J., Fang, Y., Wang, G., Liu, B., & Wang, R. (2023). The aging of farmers and its challenges for labor-intensive agriculture in China: A perspective on farmland transfer plans for farmers' retirement. *Journal of Rural Studies*, 100, 103013.
- Luo, S., Wang, C., Xi, X., Nie, S., Fan, X., Chen, H., Yang, X., Peng, D., Lin, Y., & Zhou, G. (2019). Combining hyperspectral imagery and LiDAR pseudo-waveform for predicting crop LAI, canopy height and above-ground biomass. *Ecological Indicators*, 102, 801-812.
- Malthus, T. J., Andrieu, B., Danson, F. M., Jaggard, K. W., & Steven, M. D. (1993). Candidate high spectral resolution infrared indices for crop cover. *Remote Sensing of Environment*, 46(2), 204-212.
- Mariye, M., Mariyo, M., Changming, Y., Teffera, Z. L., & Weldegebrial, B. (2022). Effects of land use and land cover change on soil erosion potential in Berhe district: A case study of Legedadi watershed, Ethiopia. *International Journal of River Basin Management*, 20(1), 79-91.

- Meena, R. K., Reddy, K. S., Gautam, R., Maddela, S., Reddy, A. R., & Gudipalli, P. (2021). Improved photosynthetic characteristics correlated with enhanced biomass in a heterotic F1 hybrid of maize (*Zea mays* L.). *Photosynthesis Research*, 147, 253-267.
- Meiyan, S., Mengyuan, S., Qizhou, D., Xiaohong, Y., Baoguo, L., & Yuntao, M. (2022). Estimating the maize above-ground biomass by constructing the tridimensional concept model based on UAV-based digital and multi-spectral images. *Field Crops Research*, 282, 108491.
- Mgbenka, R., Mbah, E., & Ezeano, C. (2016). A review of smallholder farming in Nigeria: Need for transformation. *International Journal of Agricultural Extension and Rural Development Studies*, 3(2), 43-54.
- Miura, T., Yoshioka, H., Fujiwara, K., & Yamamoto, H. (2008). Inter-comparison of ASTER and MODIS surface reflectance and vegetation index products for synergistic applications to natural resource monitoring. *Sensors*, 8(4), 2480-2499.
- Mu, C., Li, L., Zhang, F., Li, Y., Xiao, X., Zhao, Q., & Zhang, T. (2018). Impacts of permafrost on above-and belowground biomass on the northern Qinghai-Tibetan Plateau. *Arctic, Antarctic, and Alpine Research*, 50(1), e1447192.
- Muruganantham, P., Wibowo, S., Grandhi, S., Samrat, N. H., & Islam, N. (2022). A Systematic Literature Review on Crop Yield Prediction with Deep Learning and Remote Sensing. *Remote sensing*, 14(9), 1990. <https://www.mdpi.com/2072-4292/14/9/1990>
- Ndlovu, H. S., Odindi, J., Sibanda, M., Mutanga, O., Clulow, A., Chimonyo, V. G., & Mabhaudhi, T. (2021). A comparative estimation of maize leaf water content using machine learning techniques and unmanned aerial vehicle (UAV)-based proximal and remotely sensed data. *Remote sensing*, 13(20), 4091.
- Ngoune Tandzi, L., & Mutengwa, C. S. (2019). Estimation of maize (*Zea mays* L.) yield per harvest area: Appropriate methods. *Agronomy*, 10(1), 29.
- Niu, Y., Zhang, L., Zhang, H., Han, W., & Peng, X. (2019). Estimating above-ground biomass of maize using features derived from UAV-based RGB imagery [Article]. *Remote Sensing*, 11(11), Article 1261. <https://doi.org/10.3390/rs11111261>
- Odebiri, O., Mutanga, O., Odindi, J., Naicker, R., Masemola, C., & Sibanda, M. (2021a). Deep learning approaches in remote sensing of soil organic carbon: A review of utility, challenges, and prospects. *Environmental Monitoring and Assessment*, 193, 1-18.
- Odebiri, O., Mutanga, O., Odindi, J., Naicker, R., Masemola, C., & Sibanda, M. (2021b). Deep learning approaches in remote sensing of soil organic carbon: a review of utility, challenges, and prospects. *Environmental Monitoring and Assessment*, 193(12), 802. <https://doi.org/10.1007/s10661-021-09561-6>
- Olson, D., & Anderson, J. (2021). Review on unmanned aerial vehicles, remote sensors, imagery processing, and their applications in agriculture. *Agronomy Journal*, 113(2), 971-992.
- Onyango, C. M., Nyaga, J. M., Wetterlind, J., Söderström, M., & Piikki, K. (2021). Precision agriculture for resource use efficiency in smallholder farming systems in sub-saharan africa: A systematic review. *Sustainability (Switzerland)*, 13(3), 1158.
- Palacios-Rojas, N., McCulley, L., Kaeppler, M., Titcomb, T. J., Gunaratna, N. S., Lopez-Ridaura, S., & Tanumihardjo, S. A. (2020). Mining maize diversity and improving its nutritional aspects within agro-food systems. *Comprehensive Reviews in Food Science and Food Safety*, 19(4), 1809-1834.
- Peter, B. G., Messina, J. P., Carroll, J. W., Zhi, J., Chimonyo, V., Lin, S., & Snapp, S. S. (2020). Multi-spatial resolution satellite and sUAS imagery for precision agriculture on smallholder farms in Malawi. *Photogrammetric Engineering & Remote Sensing*, 86(2), 107-119.

- Polzin, M., & Hughes, J. (2023). Automation in steep terrain agriculture: an optimal controller to prevent tipping and slipping of tethered robots on slopes. *Advanced Robotics*, 37(15), 987-998.
- Salem, H., Kabeel, A., El-Said, E. M., & Elzeki, O. M. (2022). Predictive modelling for solar power-driven hybrid desalination system using artificial neural network regression with Adam optimization. *Desalination*, 522, 115411.
- Salinas-Melgoza, M. A., Skutsch, M., & Lovett, J. C. (2018). Predicting aboveground forest biomass with topographic variables in human-impacted tropical dry forest landscapes. *Ecosphere*, 9(1), e02063. <https://doi.org/10.1002/ecs2.2063>
- Saranya, T., Deisy, C., Sridevi, S., & Anbananthen, K. S. M. (2023). A comparative study of deep learning and Internet of Things for precision agriculture. *Engineering Applications of Artificial Intelligence*, 122, 106034.
- Sharma, P., Leigh, L., Chang, J., Maimaitijiang, M., & Caffé, M. (2022). Above-ground biomass estimation in oats using UAV remote sensing and machine learning. *Sensors*, 22(2), 601.
- Shi, H., & Xingguo, M. (2011). Interpreting spatial heterogeneity of crop yield with a process model and remote sensing. *Ecological Modelling*, 222(14), 2530-2541.
- Sun, X., Yang, Z., Su, P., Wei, K., Wang, Z., Yang, C., Wang, C., Qin, M., Xiao, L., & Yang, W. (2023). Non-destructive monitoring of maize LAI by fusing UAV spectral and textural features. *Frontiers in plant science*, 14, 1158837.
- Svedin, J. D., Kerry, R., Hansen, N. C., & Hopkins, B. G. (2021). Identifying within-field spatial and temporal crop water stress to conserve irrigation resources with variable-rate irrigation. *Agronomy*, 11(7), 1377.
- Tang, Y., Zhou, R., He, P., Yu, M., Zheng, H., Yao, X., Cheng, T., Zhu, Y., Cao, W., & Tian, Y. (2023). Estimating wheat grain yield by assimilating phenology and LAI with the WheatGrow model based on theoretical uncertainty of remotely sensed observation. *Agricultural and Forest Meteorology*, 339, 109574.
- Tollenaar, M., & Lee, E. (2002). Yield potential, yield stability and stress tolerance in maize. *Field Crops Research*, 75(2-3), 161-169.
- Tripathi, A., Tiwari, R. K., & Tiwari, S. P. (2022). A deep learning multi-layer perceptron and remote sensing approach for soil health based crop yield estimation. *INTERNATIONAL JOURNAL OF APPLIED EARTH OBSERVATION AND GEOINFORMATION*, 113, 102959.
- Tsai, C.-W., & Fang, Z.-Y. (2021). An effective hyperparameter optimization algorithm for DNN to predict passengers at a metro station. *ACM Transactions on Internet Technology (TOIT)*, 21(2), 1-24.
- Tucker, C. J., Elgin Jr, J., McMurtrey Iii, J., & Fan, C. (1979). Monitoring corn and soybean crop development with hand-held radiometer spectral data. *Remote Sensing of Environment*, 8(3), 237-248.
- Vélez, S., Martínez-Peña, R., & Castrillo, D. (2023). Beyond Vegetation: A Review Unveiling Additional Insights into Agriculture and Forestry through the Application of Vegetation Indices. *J*, 6(3), 421-436.
- Verschuur, J., Li, S., Wolski, P., & Otto, F. E. (2021). Climate change as a driver of food insecurity in the 2007 Lesotho-South Africa drought. *Scientific reports*, 11(1), 3852.
- Vojnov, B., Jaćimović, G., Šeremešić, S., Pezo, L., Lončar, B., Krstić, Đ., Vujić, S., & Čupina, B. (2022). The effects of winter cover crops on maize yield and crop performance in semiarid conditions—artificial neural network approach. *Agronomy*, 12(11), 2670.

- Wang, F.-M., HUANG, J.-f., TANG, Y.-l., & WANG, X.-z. (2007). New vegetation index and its application in estimating leaf area index of rice. *Rice Science*, 14(3), 195-203.
- Wang, X., Ren, H., & Wang, A. (2022). Smish: A novel activation function for deep learning methods. *Electronics*, 11(4), 540.
- Wang, Y., Xiao, Z., & Cao, G. (2022). A convolutional neural network method based on Adam optimizer with power-exponential learning rate for bearing fault diagnosis. *Journal of Vibroengineering*, 24(4), 666-678.
- Wu, C., Niu, Z., Tang, Q., & Huang, W. (2008). Estimating chlorophyll content from hyperspectral vegetation indices: Modeling and validation. *Agricultural and Forest Meteorology*, 148(8-9), 1230-1241.
- Yang, B., Zhu, W., Rezaei, E. E., Li, J., Sun, Z., & Zhang, J. (2022). The optimal phenological phase of maize for yield prediction with high-frequency UAV remote sensing. *Remote sensing*, 14(7), 1559.
- Yang, H., Ming, B., Nie, C., Xue, B., Xin, J., Lu, X., Xue, J., Hou, P., Xie, R., & Wang, K. (2022). Maize Canopy and Leaf Chlorophyll Content Assessment from Leaf Spectral Reflectance: Estimation and Uncertainty Analysis across Growth Stages and Vertical Distribution. *Remote Sensing*, 14(9), 2115.
- Yue, J., Yang, H., Yang, G., Fu, Y., Wang, H., & Zhou, C. (2023). Estimating vertically growing crop above-ground biomass based on UAV remote sensing. *Computers and Electronics in Agriculture*, 205, 107627.
- Zeng, Y., Hao, D., Huete, A., Dechant, B., Berry, J., Chen, J. M., Joiner, J., Frankenberg, C., Bond-Lamberty, B., & Ryu, Y. (2022). Optical vegetation indices for monitoring terrestrial ecosystems globally. *Nature Reviews Earth & Environment*, 3(7), 477-493.
- Zeng, Z., Yao, Y., Liu, Z., & Sun, M. (2022). A deep-learning system bridging molecule structure and biomedical text with comprehension comparable to human professionals. *Nature communications*, 13(1), 862.
- Zhai, W., Li, C., Cheng, Q., Mao, B., Li, Z., Li, Y., Ding, F., Qin, S., Fei, S., & Chen, Z. (2023). Enhancing Wheat Above-Ground Biomass Estimation Using UAV RGB Images and Machine Learning: Multi-Feature Combinations, Flight Height, and Algorithm Implications. *Remote Sensing*, 15(14), 3653.
- Zhang, H., Zhao, S., Song, Y., Ge, S., Liu, D., Yang, X., & Wu, K. (2022). A deep learning and Grad-Cam-based approach for accurate identification of the fall armyworm (*Spodoptera frugiperda*) in maize fields. *Computers and Electronics in Agriculture*, 202, 107440.
- Zhang, Y., Xia, C., Zhang, X., Cheng, X., Feng, G., Wang, Y., & Gao, Q. (2021). Estimating the maize biomass by crop height and narrowband vegetation indices derived from UAV-based hyperspectral images. *Ecological Indicators*, 129, 107985. <https://doi.org/https://doi.org/10.1016/j.ecolind.2021.107985>